Published in final edited form as:
Cancer Res. 2013 September 15; 73(18): 5719–5729. doi:10.1158/0008-5472.CAN-13-0021.

Epimorphin is a novel regulator of the progesterone receptor isoform-A

Jamie L. Bascom[*,1], **Derek C. Radisky**[2], **Eileen Koh**[1], **Jimmie E. Fata**[3], **Alvin Lo**[1], **Hidetoshi Mori**[1], **Neda Roosta**[1], **Yohei Hirai**[4], and **Mina J. Bissell**[1,*]

[1]Life Science Division, Lawrence Berkeley National Laboratory, 1 Cyclotron Road, Berkeley, CA 94720, USA

[2]Mayo Clinic Cancer Center Griffin Cancer Research Building, 4500 San Pablo Road, Jacksonville, FL 32224,USA

[3]College of Staten Island City, University of New York, 2800 Victory Boulevard Staten Island, NY, 10314, USA

[4]Dept. Bioscience, Kwansei Gakuin University, 2-1 Gakuen, Sanda 669-1337, Japan

Abstract

Epimorphin/syntaxin-2 is a membrane-tethered protein localized extracellularly (Epim) and intracellularly (Stx-2). The extracellular form Epim stimulates morphogenic processes in a range of tissues, including in murine mammary glands where its overexpression in luminal epithelial cells is sufficient to drive hyperplasia and neoplasia. We analyzed wap-Epim transgenic mice to gain insight into how Epim promotes malignancy. Ectopic overexpression of Epim during postnatal mammary gland development led to early side-branching onset, precocious bud formation and increased proliferation of mammary epithelial cells. Conversely, peptide-based inhibition of Epim function reduced side-branching. Since increased side-branching and hyperplasia occurs similarly in mice upon overexpression of the progesterone receptor isoform-a (Pgr-a), we investigated whether Epim exhibits these phenotypes through Pgr modulation. Epim overexpression indeed led to a steep upregulation of both total Pgr mRNA and Pgr-a protein levels. Notably, the Pgr antagonist, RU486, abrogated Epim-induced ductal side-branching, mammary epithelial cell proliferation and bud formation. Evaluation of Epim signaling in a 3D ex vivo culture system showed that its action was dependent on binding to its extracellular receptor, integrin-av, and on matrix metalloproteinase 3 activity downstream of Pgr-a. These findings elucidate a hitherto unknown transcriptional regulator of Pgr-a, and shed light on how overexpression of Epim leads to malignancy.

[*]Corresponding authors: Mina J. Bissell, Ph.D., Jamie L. Bascom, Ph.D., Life Sciences Division, Lawrence Berkeley National Laboratory, 1 Cyclotron Road, Berkeley, CA 94720, USA, Phone: 510-486-4365, mjbissell@lbl.gov, jlbascom@lbl.gov.

Authors Contributions

J.L.B. contributed to all of the experiments herein, critically analyzed the data, and drafted the manuscript; D.C.R. synthesized recombinant Epim protein, critically analyzed the data, and drafted the manuscript; E.K. contributed to the qPCR, immunohistochemistry, and western blotting experiments; J.E.F. contributed to transgenic animal wholemount analysis, histological analysis and critically analyzed the data; H.M. contributed to organogenesis assays, qPCR experiments and critically analyzed the data; A.T.L. assisted with mouse breeding, genotyping and isolation of mammary tissue from mice; Y.H. generated the construct for the Epim transgenic mice and the SSH peptide; M.J.B. critically analyzed the data and drafted the manuscript. All authors read and approved the final manuscript.

Conflict-of-interest disclosure: The authors declare no competing financial interests.

Keywords

Epimorphin; Progesterone receptor; mammary gland; branching morphogenesis; breast cancer

Introduction

The mouse mammary gland is a reticulum of branching tubules and alveolar structures that undergoes most of its development postnatally. Stages of development involve branching morphogenesis that commences at puberty, functional differentiation in pregnancy and lactation, and involution of alveolar structures after weaning. These stages are reproduced during estrous cycles albeit to a less dramatic extent. Endocrine hormones such as 17β-estradiol, progesterone, prolactin and glucocorticoids are essential for normal mammary gland development (reviewed in (1). Genetic ablation of the receptors for 17β-estradiol and progesterone, Esr1 and Pgr, in mice, revealed that Esr1 is required for ductal elongation whereas Pgr is critical for alveologenesis to ensue (reviewed in (2)). Through Esr1 and Pgr activation, signals for mammary gland development are propagated by upregulation of transcription factors and release of local factors. Examples of local factors include epidermal growth factor and keratinocyte growth factor for Esr1 (reviewed in (3)), and receptor activated NF-κB ligand (RANKL) for Pgr (4), and Esr1 is a primary transcriptional regulator of Pgr in the mammary gland (5). Here, we have made the surprising discovery that Pgr expression is also regulated transcriptionally by the local mammary morphogen, Epim.

Epim was first identified as a surface mesenchymal protein that was crucial for dermal and lung epithelial cell morphogenesis (6). Subsequently, Epim was rediscovered as a member of a family of integral membrane proteins renamed syntaxins (7) that were shown to have important intracellular functions in membrane fusion and exocytosis (reviewed in (8)). However, because of the distinct extracellular function of Epim, which was discovered prior to the syntaxin nomenclature and function, we continue to refer to the extracellular form as Epim and the intracellular function as Stx-2 (9, 10). Epim has been shown to regulate morphogenesis in a range of tissues including bile duct, intestinal crypts, hair follicle, skin, pancreas, gall bladder, testes, and lung, as well as in the mammary gland (reviewed in (10)). Epim is expressed in the mouse mammary gland by fibroblasts and myoepithelial cells in virgin mice (11), and additionally in luminal epithelial cells in pregnant and lactating mice (unpublished data). In three-dimensional (3D) collagen gel assays, we showed that Epim stimulated mammary epithelial cell branching and lumen formation (11-13), and that these Epim functions were dependent upon binding to its cell surface receptor, integrin-αv (14). WAP-Epim transgenic mice (15) develop thickened mammary ducts, upregulate the transcription factor CCAAT enhancer binding protein β (Cebpb) in pregnancy and develop hyperplasia and neoplasia at approximately 18-months post-birth (16).

In order to determine why WAP-Epim mice are prone to mammary hyperplasia and neoplasia after one year of birth, we asked whether these mice exhibit histological stages of cancer progression even earlier in life. We hypothesized that by analyzing young mice we could identify which molecular pathways become deregulated during this progression. We found that these mice develop also extensive lateral branches in nulliparous mice (week 8) and precocious alveolar structures in young pregnant mice (week 12) and increased mammary epithelial cell proliferation during alveologenesis. These phenotypes resembled those described for Pgr-a transgenic mice (17). In addition, WAP-Epim mice develop hyperplasia similar to Pgr-a transgenic mice. Because of the similarities between Epim and Pgr-a transgenic mice(16-19), and the fact that both Epim and Pgr upregulate Cebpb (15, 20, 21) we reasoned that there was a connection between the two molecules.

Interrogation of a downstream mechanism in both WAP-Epim transgenic mice and the ex-vivo 3D assays showed that Epim indeed regulates Pgr-a, and that Epim controls Pgr-induced side-branching, bud formation and epithelial cell proliferation. We show also that Epim regulation of Pgr-a expression occurs through activation of integrin-αv. Furthermore we show that Epim-induced proliferation and bud formation, which we showed previously to correlate with *Mmp3* expression, occurs downstream of Pgr.

Materials and Methods

Transgenic mice

The generation of hemizygous WAP-Epim mice (abbreviated further as TG in figures), in which Epim is tagged with the mouse IL-2 signal peptide sequence and expressed under control of the whey acidic protein promoter, has been described previously (15). Transgene-negative littermates were used as controls. Animal use protocols were obtained and procedures were followed in strict accordance with guidelines established by the Lawrence Berkeley National Laboratory Animal Welfare and Research Committee (AWRC).

Staging of developmental time points

Nulliparous mice were analyzed at 1.5, 8, and 14-weeks after birth. For analysis of alveolar development, tissue was collected from pregnant WT and WAP-Epim animals at day 12 of pregnancy. To stage pregnancy, breeding mice were checked in the A.M. for vaginal plugs. If plugs were found, the female was separated from the male and this day was designated day 0 of pregnancy. For analysis of lactation, dams were allowed to nurse 6 pups to equalize suckling, tissue was collected on day 10 subsequent to parturition.

Tissue collection and wholemounts

At the time of dissection, the stage of estrous was determined by vaginal lavage followed by cytological analysis. For each study, the thoracic and inguinal mammary glands were excised and frozen immediately on dry ice for RNA and protein isolation or they were formalin fixed for histological analysis. One inguinal gland was fixed in Carnoy's solution overnight then stained with carmine alum to analyze ductal/alveolar morphology.

Genotyping, reverse transcriptase (RT) and polymerase chain reaction (PCR)

For genotyping, tail DNA was digested overnight in 50μl proteinase K buffer, diluted 8× and used as template for PCR reaction. The expression of the Epim transgene was confirmed by RT-PCR. For analysis of gene expression in mouse mammary glands, total RNA was extracted from frozen mammary glands using TRIzol ® (Invitrogen, Carlsbad, CA) or from mammary organoids using an RNeasy kit (Qiagen, Valencia, CA) then reverse transcribed using Superscript II First Strand Synthesis System (Invitrogen, Carlsbad, CA). qPCR was performed using a LightCycler ® (Roche Diagnostics, Indianapolis, IN). Primers used in qPCR reactions are listed in table 1 in the supplementary material.

Histological analysis

Histomorphometry to compare differences in epithelial density was performed using a Mertz graticule on H&E stained 5μm mammary gland paraffin sections generated by the UCSF Helen Diller Family Comprehensive Cancer Center Mouse Pathology Core. Five successive fields were examined for each mammary gland. The criteria included the presence or absence of epithelial structures or adipocytes. To quantify side-branching, the three longest ducts were analyzed on each mammary gland wholemount beginning from the lymph node. The number of side-branches was divided by the length to yield side-branches/branch-length.

Protein isolation

From each animal, thoracic mammary glands were homogenized in 500 μL lysis buffer (10mM Tris [pH 7.6], 5mM EDTA, 50mM NaCl, 1% Triton-X) with 1× proteinase inhibitor cocktail I (CalBiochem, Merck KGaA, Darmstadt, Germany) for immunoblotting. The homogenates were centrifuged at 12,000 *g* for 20 minutes at 4°C, supernatant was isolated and stored at −70°C until needed. Protein was isolated from organoids as previously described (22). Protein concentration was determined using Biorad DC protein assay reagents (Bio-Rad Laboratories Inc., Hercules, CA).

Western Analysis

For western analysis, 10 μg protein lysate was added to loading buffer (250 mM Tris-HCl pH 6.8, 10% SDS, 20% β-mercaptoethanol, 40% glycerol), boiled for 5 minutes, and electrophoresed on 12% polyacrylamide gels (Invitrogen, Carlsbad, CA). After transferring onto nitrocellulose membranes .45 μm (Bio-Rad Laboratories Inc. Hercules, CA), total blotted protein was visualized by PonceauS staining. Blots were blocked overnight at 4°C using 5% nonfat dry milk in 1× tris-buffered saline. Antibodies against β-casein, generated from hybridoma cells in the Bissell Lab used at a 1/10,000 dilution to test functional differentiation (23), the beta-catenin mouse monoclonal antibody was from Sigma (C-7207, St. Louis, MO), the Pgr antibody (Ab-8, Neomarkers, Fremont, CA), and lamin A/C (Lmna) and estrogen receptor antibodies were from Santa Cruz Biotechnology (H-110 and MC-20, Santa Cruz, CA). Secondary horse radish peroxidase (HRP) conjugated anti-mouse and anti-rabbit antibodies were from Amersham Biosciences (GE Healthcare, Piscataway, NJ). Dilutions followed manufacturers' suggestion. Detection of HRP signal was achieved using Thermoscientific Supersignal West Dura (Asheville, NC) with a FluorChem™ 8900 chemical imager (Alpha Innotech, Cell Biosciences, Santa Clara, CA).

Immunostaining on mammary sections

Mammary sections (5 μm) were deparaffinized and rehydrated in graded alcohol to 1× PBS, then blocked for 10 minutes in 3% H_20_2 in 70% ethanol, followed by antigen retrieval for 10 minutes in sodium citrate buffer (10 mM sodium citrate, pH 6.0) using a microwave. Slides were incubated overnight in a humidified chamber with anti-Epim 1/50 dilution (MC-1 antibody, gift from Y. Hirai), anti-Cebpb at a 1/100 dilution (Santa Cruz Biotechnology, Santa Cruz, CA), anti-cyclin D1(Ccnd1) at a 1/100 dilution (Thermoscientific, Rockford, IL), and anti-Pgr at a 1/50 dilution (DAKO, Carpinteria, CA) then washed in 1× PBS and incubated for 1-hour with biotinylated secondary antibodies. Avidin:Biotinylated enzyme complex (ABC kit, Vector Laboratories, Burlingame, CA) was used to amplify signal, followed by visualization using 3, 3′-diaminobenzidine (DAB) color substrate (Sigma, St. Louis, MO).

Statistical analysis

To determine statistical significance, two-tailed paired T-Tests were used when treatments were to organoids or tissue from the same animal. For comparing differences in expression or morphology between various mice two-tailed Mann Whitney tests were used. A P-value of less than .05 was considered significant. All error bars represent standard error (s.e.m.) measurements.

Results

Epim controls the level of side-branching in the nulliparous mouse mammary gland

We reported previously that WAP-Epim transgenic mice develop alveolar hyperplasia and adenocarcinoma with high incidence when they age to approximately 18 months; however,

we did not know the molecular mechanism by which Epim overexpression could cause mammary tumors. To determine the mechanism(s) leading to malignancy, we investigated whether there were consequences to mammary gland development when Epim signaling becomes deregulated. To inhibit Epim, we utilized Pep7, a ten-amino acid peptide initially discovered to be the minimal portion of the H1 domain of Epim capable of inducing a telogen-to-anagen transition in mouse hair follicle morphogenesis (24), and that was found also to inhibit Eph4 mammary epithelial cell branching in collagen gels (25). We injected pep7, or a control scrambled peptide, into the contra-lateral mammary glands of WT mice and observed a significant decrease in side-branching in pep7-injected mammary glands as compared to glands injected with control peptide (Figure 1A,B). We did not, however, observe any difference in ductal length between pep7-treated mammary glands and contralateral scramble peptide-treated glands (not shown). Pgr is necessary also for side-branching but not ductal length in the mouse mammary gland (26). That we observed a decrease in side-branching but not ductal-length when using the Epim inhibitor suggested that Pgr might be involved. Thus, we proceeded to analyze young WAP-Epim transgenic mice to determine whether there are similar defects in ductal development as in Pgr transgenic mice.

While the promoter of the WAP gene is activated most strongly from day ten of pregnancy through lactation, with residual activity during involution (27), WAP is expressed also in nulliparous mice (28) and we observed upregulated Epim in the mammary epithelial cells of nulliparous WAP-Epim mice (Fig 1C), associated with an increased ratio of epithelial cells (E) compared to adipocytes (A) as compared to the WT (~80% increased) (Figure 1D). To evaluate how overexpression of Epim affected ductal outgrowth, mammary glands were isolated before, during and after peak ductal outgrowth at 1.5, 8 and 14 weeks. At 1.5 weeks, WAP-Epim mammary glands were indistinguishable from WT in terms of ductal length and the number of primary branches ($n=10$, not shown). To control for hormonal differences between cycling 8 and 14 week old WT and transgenic (TG) mice, they were compared only in the same estrous stage. By 8 weeks of age, mammary glands from WAP-Epim mice showed ~80% more side-branches than the WT (Figure 1E,F). In contrast, there were no statistical differences in ductal-length (Figure S1A). By 14 weeks, the WT mammary gland had caught up in the number of side-branches compared to the WAP-Epim mouse ($n=11$ WT, $n=19$ TG, not shown).

As a further control for the specificity of Epim action to induce side branching, we compared the effect of a recombinant soluble Epim to that of an engineered protein which is 82% homologous to Epim (rStx1a), but that does not activate Epim responses in culture (29). Using the same mouse, we injected rEpim peptide to one inguinal mammary gland and rStx1a peptide to the contralateral mammary gland. Whereas there were no significant differences in number of side-branches or ductal-length between the right and left inguinal mammary glands injected with PBS alone (not shown), the rEpim injected mammary gland showed a significant increase in side-branches compared to the rStx1a treated contralateral side in the same mouse (Figure 1G). Again, we did not observe a difference in ductal-length as was the case also between WAP-Epim and WT mice, and the case between pep7 and mammary glands treated with scrambled peptides. Thus attenuating Epim signaling early in ductal development hinders the elaboration of secondary branches, whereas overexpression of Epim stimulates precocious side-branching without affecting ductal length. These phenotypes resemble both the defect in side-branching in the Pgr knockout mice (26, 30) and the supernumerary side-branching and hyperplasia in the Pgr-a transgenic mice (17).

Epim overexpression stimulates precocious alveologenesis through upregulation of Pgr in pregnancy

Administration of 17-β estradiol and progesterone to mice where both Pgr isoforms were ablated showed that Pgr is necessary for alveolar differentiation in the mouse mammary gland (26). Given that WAP-Epim mice show also increased side-branching, ductal ectasia and hyperplasia similar to the Pgr-a transgenic mice (17, 18), we hypothesized that the action of Pgr to induce alveologenesis during pregnancy could be regulated also by Epim. Whole mounts and histological sections of WT and WAP-Epim mammary glands showed a dramatic increase in the number of alveolar structures at day 12 of pregnancy compared to WT (Figure 2A, B), a time point at which Epim was highly overexpressed in the WAP-Epim mammary gland (Figure 2C). WAP-Epim mammary glands displayed larger, more abundant alveoli with larger lumena, increased lipid droplets (Figure 2B, arrow) and elevated beta casein expression (not shown) compared with WT. We reported previously that mammary glands from pregnant WAP-Epim mice developed enlarged mammary ducts (15), a phenotype observed also in the Pgr-a transgenic mice (17).

Esr1 is a well-known positive regulator of Pgr expression in the mammary gland (31). Therefore, we assessed whether Epim regulates Esr1 in the mouse mammary gland during midpregnancy (day 12 of gestation). We did not detect significant differences in Esr1 mRNA by qPCR (Figure 2D). However, Pgr mRNA (Figure 2E) and protein levels (Figure 2F, G) were significantly elevated in the TG mice compared to WT. Using a polyclonal antibody that detects both isoforms, we showed that Epim predominately regulates Pgr-a (Figure 3F,G; band at 80 Kda for Pgr-a is compared to one at 110 Kda corresponding to Pgr-b), indicating that Epim regulates primarily Pgr-a. Therefore, the effects of Epim on ductal elongation and alveolar differentiation are consistent with the distinct effects of Esr1 and Pgr on these processes and the differential expression of Esr1 and Pgr-a in the WAP-Epim transgenic mouse mammary glands.

Precocious side-branching in the WAP-Epim transgenic mammary gland is driven by Pgr-a

In nulliparous WAP-Epim mice, we observed also a sharp increase in Pgr immunoreactivity compared to WT by immunohistochemistry (Figure 3A, C). Additionally, Pgr expression was less heterogeneous compared to WT, often showing clustered expression along mammary ducts (Fig 3A, WAP-Epim, arrow). We observed also upregulation of two Pgr - responsive genes (20): CCAAT enhancer binding protein b (Cebpb) (not shown) and Cyclin D1 (Ccnd1) (Fig 3B, D). Ccnd1 has been shown to be involved in the first wave of proliferation induced by progesterone in Pgr positive luminal epithelial cells (4). To test whether Pgr expression is required for stimulation of side-branching in the WAP-Epim mice, six-week old mice were injected subcutaneously with the Pgr antagonist RU486 or oil control every other day for eight days. By whole mount analysis, the RU486-treated mice showed approximately 70% fewer side-branches than controls (Figure 3E). We conclude that the effects of Pgr effects on side-branching in the mammary gland may be related to Epim regulation of Pgr-a.

Epim stimulates MEC proliferation through Pgr upregulation

Analysis of signaling cascades in vivo is complicated by the rapid development of the mammary gland, and the constantly changing composition of hormones and growth factors. To study these interactions in a more controlled microenvironment and to define further cellular mechanisms underlying Epim-driven precocious alveologenesis in the WAP-Epim mouse, we employed an ex-vivo assay established in our laboratory (22). We used fragments of mammary epithelium (‘organoids’) generated from 8-week old mice in 3D Lr-ECM. In this assay, addition of a growth factor, such as transforming growth factor alpha, initiates alveolar bud-like morphogenesis. When the epithelial fragment is embedded into Lr-ECM, it

forms a simple bi-layered cyst with a hollow lumen. A growth factor such as TGFα or fibroblast growth factor-2 stimulates epithelial cell proliferation and lumen filling, expansion of the multi-cell layered cysts, and eventually budding and ductal extension (32). Cell proliferation was shown to be required early in the process of cyst formation, approximately a day after growth factor treatment (22).

We confirmed that the Epim transgene was expressed in organoids embedded in Lr-ECM (Figure S2A). At the time of organoid isolation and embedding into Lr-ECM, there was a nonsignificant size difference between WT and WAP-Epim organoids (Figure S2E). However, one day after embedding into Lr-ECM, WAP-Epim organoids or WT organoids treated with rEpim formed larger cysts than WT or BSA controls, respectively (Figure S2D,F), indicating that Epim-TG mammary organoids grew at a faster rate than WT. This observation was made before the organoids were treated with TGFα, the growth factor that is added to initiate branching. Labeling organoids with 5-ethynyl-2′ deoxyuridine (EdU) to detect cells in S-phase showed that WAP-Epim organoids, on average, contained 2.8-fold greater number of EdU positive epithelial cells compared to WT in Lr-ECM on the first day after embedding into Lr-ECM (Figure 4A,B).

Pgr regulates alveologenesis in the mouse mammary gland (26) and we had found that Pgr activity was elevated in Epim-induced side-branching (Figure 2E,G). As Pgr also stimulates MEC proliferation (4, 33), we asked whether Epim stimulates MEC proliferation through Pgr. We observed an increase in total Pgr expression in the WAP-Epim organoids in Lr-ECM compared to WT (Figure S2B) as observed also *in vivo*. We also observed a trend for upregulation of Pgr in WT organoids treated with rEpim (Figure S2C, G), suggesting that this regulation occurs without the requirement of the WAP promoter. To test whether Epim controls MEC proliferation through Pgr, we treated WT and WAP-Epim mammary glands in Lr-ECM with RU486 and found that this treatment abrogated the increased proliferation in WAP-Epim organoids (Figure 4A,B). Additionally, we found that increased bud formation in WAP-Epim organoids was blocked also by RU486 (Figure 4C, D), implicating an Epim-Pgr signaling axis in both proliferation and bud formation.

Epim was shown previously to induce MEC branching in a 3D collagen gel culture assay through upregulation of matrix metalloproteinases (MMP) (12), and to increase hepatocellular carcinoma invasion and metastasis through activation of MMP9 (34). Here, we found also that WAP-Epim mice upregulate *MMP3* and *MMP9* (Figure 5A,B). We hypothesized that MMP activity is required for increased proliferation and bud formation in mammary glands of WAP-Epim mice. To test this, we used the broad spectrum chemical inhibitor of MMP activity, GM6001, and found this indeed to be true (Figure 5C-E). We also tested whether Pgr activity regulates MMPs in this context by treating WT and WAP-Epim organoids with RU486 and analyzed MMP expression by qPCR. RU486 treatment down regulated *MMP3* (Figure 5F) but not *MMP9* (not shown) in both WT and WAP-Epim organoids. *MMP2* has been shown previously to signal downstream of Pgr in Pgr-a transgenic mice (18). Our results demonstrate that Epim-stimulated *MMP3* expression is also downstream of Pgr in WAP-Epim mice.

WAP-Epim transgenic mice stimulate Pgr expression and bud formation via integrin alpha-v

We asked whether integrin-αv, known to bind to Epim to elicit downstream responses in 3D-collagen gels (13), was required to stimulate precocious bud formation in WAP-Epim mice. Treatment of organoids in the ex vivo 3D Lr-ECM assay with integrin function blocking antibodies against integrin-αv or IgG control did not show any morphological differences when induced with TGFα (Figure 6A, C). In contrast, WAP-Epim mammary organoids treated with integrin-αv inhibitory antibodies showed a 50% decrease in the

number of organoids with more than 3 alveolar buds compared to the anti-IgG-treated control antibody (Figure 6A, C). Chemical inhibitors of the mitogen-activated protein kinase and the phosphoinositide-3-kinase pathways, downstream of integrin-αv, were even more potent inhibitors of alveolar development and proliferation in both WT and WAP-Epim transgenic mice (Figure 6B and D). Finally we showed that Epim controls Pgr expression through activation of integrin-αV after by downregulation of Pgr expression following treatment with the inhibitor of integrin-αv (Figure 6E).

Discussion

In this manuscript, we have defined a role for Epim in postnatal formation of the mammary gland. We found that overexpression of exogenous Epim or introduction of a recombinant Epim peptide lead to precocious side-branching and bud formation in nulliparous mice. We found also that a peptide inhibitor of Epim decreased side-branching in WT mice. Since WAP-Epim mice eventually develop mammary carcinoma, these results suggest that Epim-induced precocious mammary gland development may be a factor predisposing these mice to mammary cancer later in life.

We believe this is the first demonstration that Epim is a regulator of Pgr-a expression. In the mouse mammary gland, regulation is through integrin-αV. The finding could have broad clinical implications for how Pgr is regulated in the mammary gland during normal development as well as in cancer progression by molecules in the cellular microenvironment. Increased Pgr-a expression has been shown previously to be involved in mammary hyperplasia ((17, 18)) and mammary tumors in BRCA1/P53 null transgenic mice ((35)). Our results add to this literature by showing that the high propensity of mammary cancer we have reported in this WAP-Epim mouse model (16) is essentially due to increased Pgr.

Pgr is required for side-branching and alveologenesis in the mouse mammary gland (26, 36). We observed a striking increase in Pgr mRNA and protein expression in WAP-Epim mammary glands compared to WT as well as upregulation of Pgr target genes such as Ccnd1, Cebpb and keratin 14 (20) (not shown). Treatment of WAP-Epim mice with the Pgr antagonist, RU486, or addition of RU486 to the culture medium of WAP-Epim organoids reduced side-branching and alveolar bud formation significantly, demonstrating that Pgr is downstream and required for the observed Epim-induced effects.

The WAP-Epim mice share some similarities to the WAP-*Mmp3* mice, including precocious alveolar development (37) and spontaneous development of mammary cancer (16, 38, 39). The mammary glands of *Mmp3* knockout mice have decreased lateral branching without any effect on ductal length (40), similar to the phenotype we observed using the Epim inhibitor in the mouse mammary gland. Treatment with rEpim was shown to upregulate *Mmp3* in mammary organoids in 3D collagen gels (12). We found that RU486 blocked *Mmp3* expression in both WT and WAP-Epim mice showing that Pgr regulates *Mmp3* in the mouse mammary gland. These results implicate *Mmp3* as an important effector downstream of Pgr-induced processes during mammary gland development, and potentially also during mammary cancer progression.

In Brca1/P53 null mice, Pgr was shown to be upregulated, due to decreased turnover of Pgr (35). In this mouse model, upregulation of Pgr caused mammary tumor formation, and inhibition of Pgr using RU486 decreased tumor formation (35). Pgr is a well-established transcriptional target of Esr1, we did not detect differences in Esr1 mRNA or protein expression between the mammary glands of WT and WAP-Epim pregnant mice. Therefore, Epim should be included as a novel regulator of Pgr-a mRNA and protein. Additionally, our

study demonstrates that Epim-induced increase in Pgr-a expression also leads to tumor formation.

It is important to note that we observed Epim induction of Pgr *without* treating mice with either estrogen- or progesterone or adding the hormones to the organoid culture medium. There is prior evidence for unliganded Pgr activity in development and cancer processes. One mechanism for Pgr unliganded activity is through activation of MAP kinase and/or PI3kinase pathways (reviewed in: (41, 42)). Since Epim upregulates both of these pathways (13), it is likely that this could explain the mode by which Epim activates Pgr-a.

We reported previously a profound morphological difference between the mammary glands of the homozygous WAP-Epim mice and those of the wild type. Additionally, we reported that the former have difficulty nursing their pups (15). However, we did not observe any morphological differences between WT and WAP-Epim mammary glands of the hemizygous mice during lactation by whole mount and histological analysis (day 10). This included the number and size of alveolar structures (Figure S-1C). Additionally, there were no measurable differences in beta-casein expression at lactation (not shown), and WAP-Epim mice were able to support full litters (10-12 pups, on average). The absence of an obvious morphological or functional difference between wildtype and hemizygous transgenic mice at lactation is likely due to less transgene expression compared to the homozygous WAP-Epim mice. Also, serum progesterone level is known to drop precipitously at the onset of lactation and remain low throughout lactation (reviewed in: (43)).This may diminish any effects of Epim-induced Pgr-a effects in WAP-Epim hemizygous mice at this developmental stage (15). These results further emphasize the importance of the Epim-Pgr signaling axis.

In normal adult human breast cells only 7-10% of luminal epithelial cells express PGR and ESR1. In contrast, seventy percent of breast tumors express PGR and ESR1 (41). Cells that express PGR in both normal human breast and mouse mammary gland are often growth arrested (35). However, during pregnancy the proportion of cells that express PGR are increased, often co-express CCND1, and acquire the ability to proliferate (reviewed in (41)). Whereas human breast cancers that lack ESR, PGR and HER-2 are well known to have a poor prognosis (reviewed in: (44)), breast cancers that lack ESR but express PGR have been reported to be more aggressive and have a poorer prognosis than ESR+/PGR+, ESR+/PGR−, and ESR−/PGR− breast cancers (45, 46). Our finding that Epim induces Pgr-a in the absence of Esr1 upregulation highlights a potential role for Epim in more aggressive tumors. These and other data in the literature highlight the potential danger of deregulation of Pgr and progesterone signaling in breast cancer and underscore the possibility that the culprit in many of the breast cancers may be progesterone rather than estrogen (47). It is therefore surprising that in clinical settings more attention is not paid to anti-progesterone receptor therapy since in animal models the data for tumor inhibition is indeed quite impressive (35).

Conclusions

In summary, we have shown that Epim controls mammary branching morphogenesis *in vivo* through transcriptional regulation of Pgr-a. Transgenic expression of Epim caused increased expression of Pgr-a, and inhibition of Epim *in vivo* blocked Pgr-a expression. Pgr-a activity was essential for mediating the effects of Epim on ductal side-branching, epithelial cell proliferation and bud formation. Pgr-a expression was shown to be downstream of the association of Epim with its extracellular receptor, integrin-αv, and upstream of MMP-3, a key mediator of Epim-induced branching morphogenesis. Our results also extend literature linking Pgr-a expression and mammary hyperplasia in transgenic mouse models, by showing that the high propensity for developing mammary cancer we have reported in the WAP-

Epim mouse model is essentially due to increased Pgr-a. Finally, our finding that Epim induces increased Pgr-a expression in the absence of Esr1 upregulation highlights a potential role for Epim in more aggressive, Esr1-negative breast cancers.

Supplementary Material

Refer to Web version on PubMed Central for supplementary material.

Acknowledgments

Financial support: We would like to thank Susan G. Komen for the Cure for postdoctoral fellowship awards to J.L.B. (KG080306) and to H.M (02-1591). D.C.R. is supported by the NCI (CA122086), the Susan B. Komen foundation (KG110542), and the Mayo Clinic Breast Cancer SPORE (CA116201). Y.H was supported by Grant-in Aid for Scientific Research (JSPS: KAKENHI 24590365). The work from M.J.B.'s laboratory is supported by grants from the U.S. Department of Energy, Office of Biological and Environmental Research and Low Dose Scientific Focus Area (contract no. DE-AC02-05CH1123); by National Cancer Institute (awards R37CA064786, R01CA140663, U54CA112970, U01CA143233, and U54CA143836 - Bay Area Physical Sciences–Oncology Center, University of California, Berkeley, California); by U.S. Department of Defense (W81XWH0810736); and in part by a grant from The Breast Cancer Research Foundation.

Abbreviations

Epim	Epimorphin/Syntaxin-2
Pgr	progesterone receptor
Stx-1	syntaxin-1
Csn-2	beta casein
Ctnnb1	beta catenin
Esr1	estrogen receptor
WAP-Epim	Whey acidic protein-Epimorphin transgenic mouse (in figures, WAP-Epim is further abbreviated as TG)
WT	wildtype
pep7	10-amino acid peptide of epimorphin H1 domain
Sc-pep	scrambled pep7 peptide
Cebpb	CCAAT enhancer binding protein beta
Ccnd1	cyclin d1
RU	RU486 or mifepristone
ActB	beta actin
EdU	5-ethynyl-2-deoxyuridine
Mmp3	matrix metalloproteinase 3

References

1. Brisken C. Hormonal control of alveolar development and its implications for breast carcinogenesis. J Mammary Gland Biol Neoplasia. 2002; 7:39–48. [PubMed: 12160085]
2. Shyamala G. Roles of estrogen and progesterone in normal mammary gland development insights from progesterone receptor null mutant mice and in situ localization of receptor. Trends Endocrinol Metab. 1997; 8:34–9. [PubMed: 18406784]

3. Imagawa W, Pedchenko VK, Helber J, Zhang H. Hormone/growth factor interactions mediating epithelial/stromal communication in mammary gland development and carcinogenesis. J Steroid Biochem Mol Biol. 2002; 80:213–30. [PubMed: 11897505]
4. Beleut M, Rajaram RD, Caikovski M, Ayyanan A, Germano D, Choi Y, et al. Two distinct mechanisms underlie progesterone-induced proliferation in the mammary gland. Proc Natl Acad Sci U S A. 107:2989–94. [PubMed: 20133621]
5. Nilsson S, Makela S, Treuter E, Tujague M, Thomsen J, Andersson G, et al. Mechanisms of estrogen action. Physiol Rev. 2001; 81:1535–65. [PubMed: 11581496]
6. Hirai Y, Takebe K, Takashina M, Kobayashi S, Takeichi M. Epimorphin: a mesenchymal protein essential for epithelial morphogenesis. Cell. 1992; 69:471–81. [PubMed: 1581962]
7. Bennett MK, Garcia-Arraras JE, Elferink LA, Peterson K, Fleming AM, Hazuka CD, Scheller RH. The syntaxin family of vesicular transport receptors. Cell. 1993; 74:863–73. [PubMed: 7690687]
8. Woodman PG. The roles of NSF, SNAPs and SNAREs during membrane fusion. Biochim Biophys Acta. 1997; 1357:155–72. [PubMed: 9223620]
9. Radisky DC, Hirai Y, Bissell MJ. Delivering the message: epimorphin and mammary epithelial morphogenesis. Trends Cell Biol. 2003; 13:426–34. [PubMed: 12888295]
10. Radisky DC, Stallings-Mann M, Hirai Y, Bissell MJ. Single proteins might have dual but related functions in intracellular and extracellular microenvironments. Nat Rev Mol Cell Biol. 2009; 10:228–34. [PubMed: 19190671]
11. Hirai Y, Lochter A, Galosy S, Koshida S, Niwa S, Bissell MJ. Epimorphin functions as a key morphoregulator for mammary epithelial cells. J Cell Biol. 1998; 140:159–69. [PubMed: 9425164]
12. Simian M, Hirai Y, Navre M, Werb Z, Lochter A, Bissell MJ. The interplay of matrix metalloproteinases, morphogens and growth factors is necessary for branching of mammary epithelial cells. Development. 2001; 128:3117–31. [PubMed: 11688561]
13. Hirai Y, Nelson CM, Yamazaki K, Takebe K, Przybylo J, Madden B, et al. Non-classical export of epimorphin and its adhesion to alphav-integrin in regulation of epithelial morphogenesis. J Cell Sci. 2007; 120:2032–43. [PubMed: 17535848]
14. Hirai Y, Nelson CM, Yamazaki K, Takebe K, Przybylo J, Madden B, et al. Non-classical export of epimorphin and its adhesion to alphav-integrin in regulation of epithelial morphogenesis. J Cell Sci. 2007; 120:2032–43. Epub 07 May 29. [PubMed: 17535848]
15. Hirai Y, Radisky D, Boudreau R, Simian M, Stevens ME, Oka Y, et al. Epimorphin mediates mammary luminal morphogenesis through control of C/EBPbeta. J Cell Biol. 2001; 153:785–94. [PubMed: 11352939]
16. Bascom JL, Fata JE, Hirai Y, Sternlicht MD, Bissell MJ. Epimorphin overexpression in the mouse mammary gland promotes alveolar hyperplasia and mammary adenocarcinoma. Cancer Res. 2005; 65:8617–21. [PubMed: 16204027]
17. Shyamala G, Yang X, Silberstein G, Barcellos-Hoff MH, Dale E. Transgenic mice carrying an imbalance in the native ratio of A to B forms of progesterone receptor exhibit developmental abnormalities in mammary glands. Proc Natl Acad Sci U S A. 1998; 95:696–701. [PubMed: 9435255]
18. Simian M, Bissell MJ, Barcellos-Hoff MH, Shyamala G. Estrogen and progesterone receptors have distinct roles in the establishment of the hyperplastic phenotype in PR-A transgenic mice. Breast Cancer Res. 2009; 11:R72. [PubMed: 19788752]
19. Chou YC, Uehara N, Lowry JR, Shyamala G. Mammary epithelial cells of PR-A transgenic mice exhibit distinct alterations in gene expression and growth potential associated with transformation. Carcinogenesis. 2003; 24:403–9. [PubMed: 12663498]
20. Aupperlee MD, Drolet AA, Durairaj S, Wang W, Schwartz RC, Haslam SZ. Strain-specific differences in the mechanisms of progesterone regulation of murine mammary gland development. Endocrinology. 2009; 150:1485–94. [PubMed: 18988671]
21. Jia Y, Yao H, Zhou J, Chen L, Zeng Q, Yuan H, et al. Role of epimorphin in bile duct formation of rat liver epithelial stem-like cells: involvement of small G protein RhoA and C/EBPbeta. J Cell Physiol. 2011; 226:2807–16. [PubMed: 21935930]

22. Fata JE, Mori H, Ewald AJ, Zhang H, Yao E, Werb Z, et al. The MAPK(ERK-1,2) pathway integrates distinct and antagonistic signals from TGFalpha and FGF7 in morphogenesis of mouse mammary epithelium. Dev Biol. 2007; 306:193–207. [PubMed: 17448457]
23. Xu R, Nelson CM, Muschler JL, Veiseh M, Vonderhaar BK, Bissell MJ. Sustained activation of STAT5 is essential for chromatin remodeling and maintenance of mammary-specific function. J Cell Biol. 2009; 184:57–66. [PubMed: 19139262]
24. Takebe K, Oka Y, Radisky D, Tsuda H, Tochigui K, Koshida S, et al. Epimorphin acts to induce hair follicle anagen in C57BL/6 mice. Faseb J. 2003; 17:2037–47. [PubMed: 14597673]
25. Nelson CM, Vanduijn MM, Inman JL, Fletcher DA, Bissell MJ. Tissue geometry determines sites of mammary branching morphogenesis in organotypic cultures. Science. 2006; 314:298–300. [PubMed: 17038622]
26. Lydon JP, DeMayo FJ, Funk CR, Mani SK, Hughes AR, Montgomery CA Jr. et al. Mice lacking progesterone receptor exhibit pleiotropic reproductive abnormalities. Genes Dev. 1995; 9:2266–78. [PubMed: 7557380]
27. Pittius CW, Hennighausen L, Lee E, Westphal H, Nicols E, Vitale J, et al. A milk protein gene promoter directs the expression of human tissue plasminogen activator cDNA to the mammary gland in transgenic mice. Proc Natl Acad Sci U S A. 1988; 85:5874–8. [PubMed: 2842753]
28. Robinson GW, McKnight RA, Smith GH, Hennighausen L. Mammary epithelial cells undergo secretory differentiation in cycling virgins but require pregnancy for the establishment of terminal differentiation. Development. 1995; 121:2070–90.
29. Chen CS, Nelson CM, Khauv D, Bennett S, Radisky ES, Hirai Y, et al. Homology with vesicle fusion mediator syntaxin-1a predicts determinants of epimorphin/syntaxin-2 function in mammary epithelial morphogenesis. J Biol Chem. 2009; 284:6877–84. [PubMed: 19129200]
30. Brisken C, Park S, Vass T, Lydon JP, O'Malley BW, Weinberg RA. A paracrine role for the epithelial progesterone receptor in mammary gland development. Proc Natl Acad Sci U S A. 1998; 95:5076–81. [PubMed: 9560231]
31. Shyamala G, Schneider W, Schott D. Developmental regulation of murine mammary progesterone receptor gene expression. Endocrinology. 1990; 126:2882–9. [PubMed: 2190799]
32. Ewald AJ, Brenot A, Duong M, Chan BS, Werb Z. Collective epithelial migration and cell rearrangements drive mammary branching morphogenesis. Dev Cell. 2008; 14:570–81. [PubMed: 18410732]
33. Imagawa W, Tomooka Y, Hamamoto S, Nandi S. Stimulation of mammary epithelial cell growth in vitro: interaction of epidermal growth factor and mammogenic hormones. Endocrinology. 1985; 116:1514–24. [PubMed: 3882412]
34. Jia YL, Shi L, Zhou JN, Fu CJ, Chen L, Yuan HF, et al. Epimorphin promotes human hepatocellular carcinoma invasion and metastasis through activation of focal adhesion kinase/extracellular signal-regulated kinase/matrix metalloproteinase-9 axis. Hepatology. 2011; 54:1808–18. [PubMed: 22045676]
35. Poole AJ, Li Y, Kim Y, Lin SC, Lee WH, Lee EY. Prevention of Brca1-mediated mammary tumorigenesis in mice by a progesterone antagonist. Science. 2006; 314:1467–70. [PubMed: 17138902]
36. Brisken C, Park S, Vass T, Lydon JP, O'Malley BW, Weinberg RA. A paracrine role for the epithelial progesterone receptor in mammary gland development. Proc Natl Acad Sci U S A. 1998; 95:5076–81. [PubMed: 9560231]
37. Sympson CJ, Talhouk RS, Alexander CM, Chin JR, Clift SM, Bissell MJ, et al. Targeted expression of stromelysin-1 in mammary gland provides evidence for a role of proteinases in branching morphogenesis and the requirement for an intact basement membrane for tissue-specific gene expression. J Cell Biol. 1994; 125:681–93. [PubMed: 8175886]
38. Sympson CJ, Bissell MJ, Werb Z. Mammary gland tumor formation in transgenic mice overexpressing stromelysin-1. Semin Cancer Biol. 1995; 6:159–63. [PubMed: 7495984]
39. Sternlicht MD, Lochter A, Sympson CJ, Huey B, Rougier JP, Gray JW, et al. The stromal proteinase MMP3/stromelysin-1 promotes mammary carcinogenesis. Cell. 1999; 98:137–46. [PubMed: 10428026]

40. Wiseman BS, Sternlicht MD, Lund LR, Alexander CM, Mott J, Bissell MJ, et al. Site-specific inductive and inhibitory activities of MMP-2 and MMP-3 orchestrate mammary gland branching morphogenesis. J Cell Biol. 2003; 162:1123–33. [PubMed: 12975354]

41. Lange CA. Challenges to defining a role for progesterone in breast cancer. Steroids. 2008; 73:914–21. [PubMed: 18243264]

42. Dressing GE, Hagan CR, Knutson TP, Daniel AR, Lange CA. Progesterone receptors act as sensors for mitogenic protein kinases in breast cancer models. Endocr Relat Cancer. 2009; 16:351–61. [PubMed: 19357196]

43. Lamote I, Meyer E, Massart-Leen AM, Burvenich C. Sex steroids and growth factors in the regulation of mammary gland proliferation, differentiation, and involution. Steroids. 2004; 69:145–59. [PubMed: 15072917]

44. Visvader JE. Keeping abreast of the mammary epithelial hierarchy and breast tumorigenesis. Genes Dev. 2009; 23:2563–77. [PubMed: 19933147]

45. Keshgegian AA, Cnaan A. Estrogen receptor-negative, progesterone receptor-positive breast carcinoma: poor clinical outcome. Arch Pathol Lab Med. 1996; 120:970–3. [PubMed: 12046611]

46. Nikolic-Vukosavljevic D, Kanjer K, Neskovic-Konstantinovic Z, Vukotic D. Natural history of estrogen receptor-negative, progesterone receptor-positive breast cancer. Int J Biol Markers. 2002; 17:196–200. [PubMed: 12408471]

47. Giersig C. Progestin and breast cancer. The missing pieces of a puzzle. Bundesgesundheitsblatt Gesundheitsforschung Gesundheitsschutz. 2008; 51:782–6. [PubMed: 18592338]

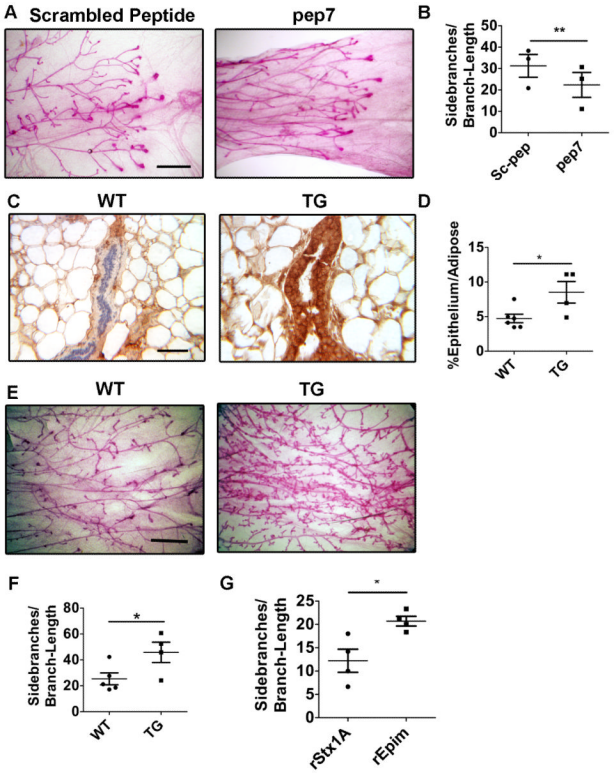

Figure 1. Epim stimulates precocious side-branching in the nulliparous mouse mammary gland

(**A,B**) Mammary gland wholemounts (**A**) and morphometric analysis (**B**) of WT mice treated with a control scramble peptide (*n=4*) or the peptide antagonist, SS7, against Epim (*n=4*) showing that blocking Epim significantly decreases side-branches. (**C**) Immunohistochemical staining of Epim expression in the luminal epithelia (brown) in mammary glands from WAP-Epim mice (TG). Nuclei are stained blue with hematoxylin. (**D**) Morphometric analysis showing that WAP-Epim mice have significantly increased ratio of epithelial cells to adipocytes compared to WT. (**E**) Mammary gland wholemount showing increased side-branching in the nulliparous 8-week old WAP-Epim mammary gland compared to the WT (*n=8* WT, *n=7* TG, metestrus stage shown). (**F**) Morphometric analysis showing significantly increased side-branching in WAP-Epim mice as compared to WT. (**G**) Morphometric analysis showing significantly increased side-branching in mammary glands injected with rEpim as compared to the control protein, rStx1a (*n=4*). Scale bar for A,E=1mm, for C=100μm. *P<0.05, **P<0.005.

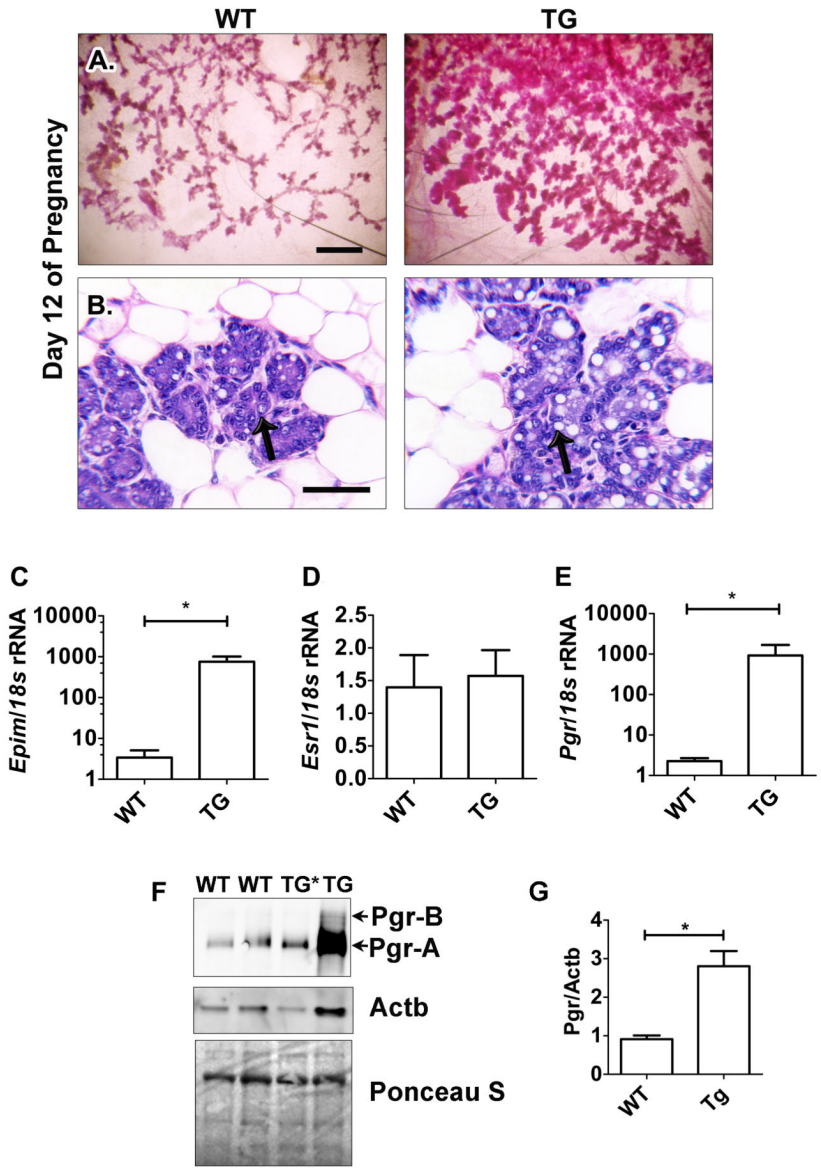

Figure 2. Epim overexpression leads to precocious alveolar development in pregnancy

(**A&B**) Wholemount and H&E stained sections at day 12 of pregnancy show increased alveolar density (**A**) and lipid droplet accumulation (**B**) in the mammary gland of WAP-Epim mice compared to WT (*n=3* WT, *n=8* TG). (**C-E**) Graphs show qPCR data for *Epim* (**C**) *Esr1* (**D**) and *Pgr* (**E**) in the WAP-Epim compared to WT. (**F**) A representative western blot shows upregulation of Pgr-A (approximately 80 Kda) in WAP-Epim mice compared to WT; Actb (beta actin) is the loading control. (**G**) Graph of Pgr densitometry normalized to Actb shows that WAP-Epim mammary glands upregulate Pgr-a compared to WT. Scale bar=1mm for A, 100μm for B. *P<0.05

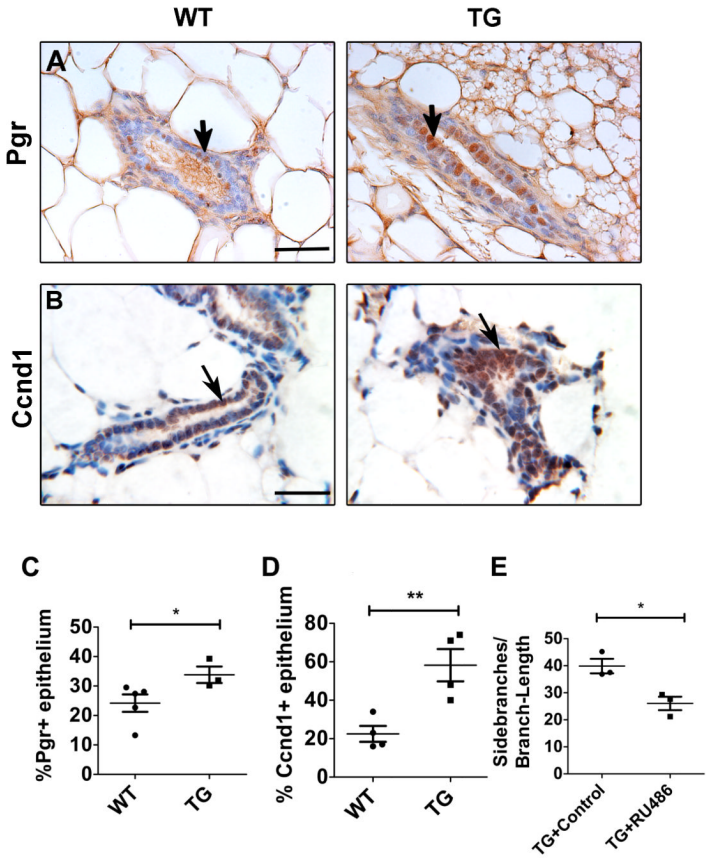

Figure 3. Precocious side-branches in WAP-Epim nulliparous mice are driven by Pgr

(**A,B**) Immunohistochemical staining shows increased Pgr immunoreactivity (**A**; *n=4* WT, *n=3* TG) and downstream target (**B**) Ccnd1 (arrows, *n=4)* in the nulliparous 8-week old mouse mammary gland. Nuclei are stained blue with hematoxylin. (**C,D**) Graphs show that the percentage of Pgr (**C**) and Ccnd1 (**D**) positive epithelial cells is greater in the WAP-Epim compared to WT. (**E**) Wholemount analysis showing decreased side-branching in WAP-Epim mammary glands injected with RU486 compared to control (*n=3*, *n=4*, respectively). Scale bar=50μm for A and 40μm for B. *P<0.05, **P<0.005.

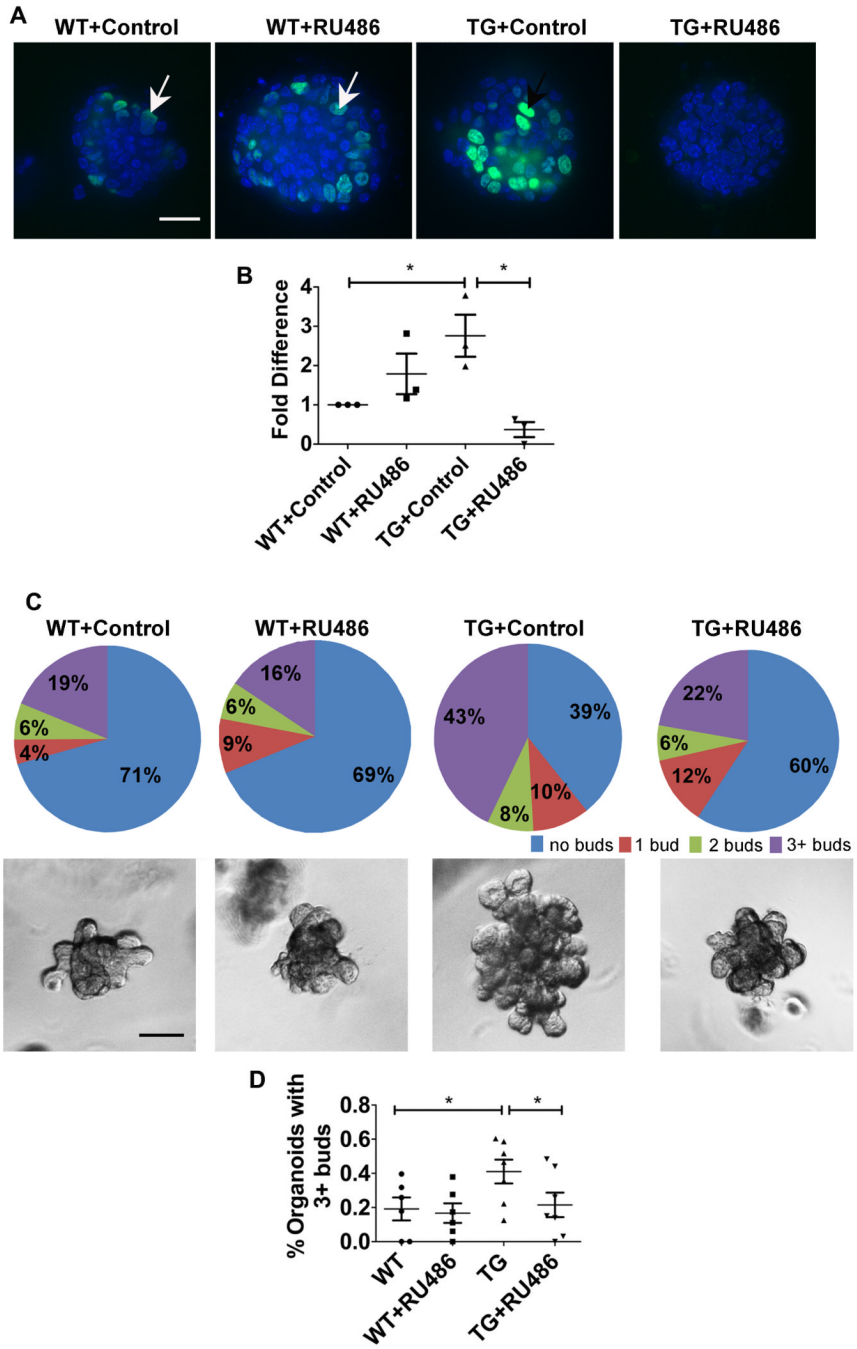

Figure 4. Epim stimulates mammary epithelial proliferation and budding through Pgr

(**A&B**) Representative images (**A**) and graph **(B)** showing increased EdU incorporation (EdU in green, indicated by arrows; DAPI in blue) in WAP-Epim organoids compared to WT on day one after embedding in Lr-ECM (*n=3*). (**C-D**) Pie charts (**C**, top), representative images (**C**, bottom), and graph (**D**) showing increased buds in the WAP-Epim mammary organoids compared to WT after treatment with 9 nM TGFα for 5 days of culture (*n=7*). *P<0.05. Bar =25 μm for A, 15 μm for C.

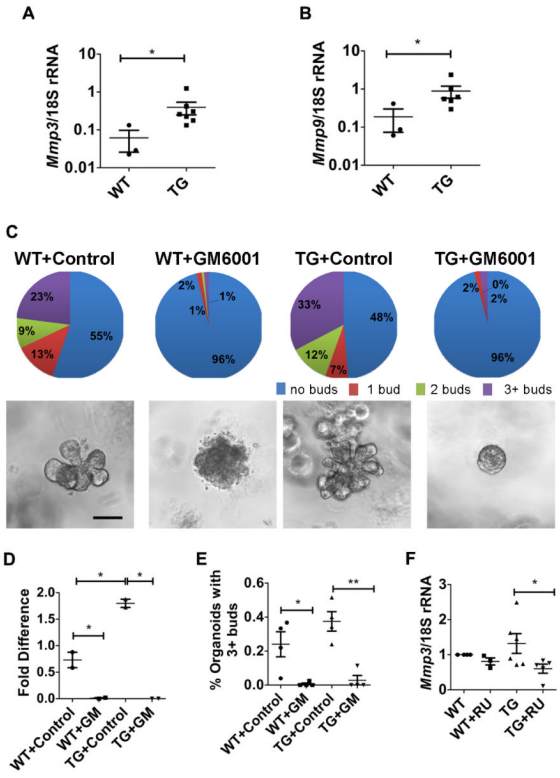

Figure 5. Precocious bud formation and proliferation in WAP-Epim mice requires MMP activity downstream of Pgr

(**A&B**) qPCR results showing upregulation of *Mmp3* (**A**) and *Mmp9* (**B**) in WAP-Epim mammary glands compared to WT in pregnancy. (**C**) Pie charts (top) and representative images (bottom) show increased bud formation in the WAP-Epim compared to WT, and that WT and WAP-Epim mice show complete inhibition of bud formation when treated with GM (*n=4*). (**D**) Quantification of EdU incorporation in WAP-Epim organoids compared to WT embedded for one day in Lr-ECM. (**E**) Both the WT and the WAP-Epim TG show decreased percentage of organoids with 3 or more buds after treatment with the MMP inhibitor. (**F**) Graph showing that *Mmp3* upregulation in the WAP-Epim mammary gland is abrogated by the Pgr antagonist RU486, demonstrating that *Mmp3* activation is downstream of Epim and Pgr. Scale bar is 25μm. *P<0.05, **P<0.005.

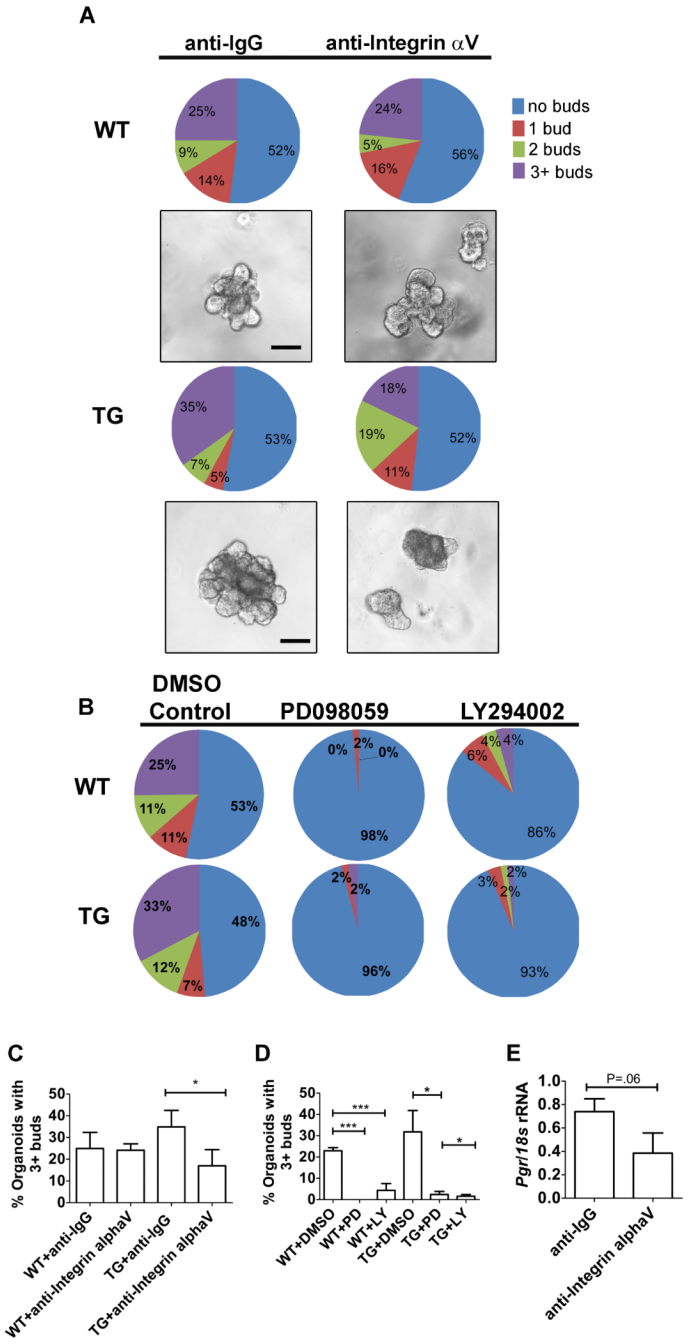

Figure 6. Integrin αV function is required for Pgr upregulation and precocious bud formation in WAP-Epim mice

(**A**) Representative phase images and pie charts showing that alveolar buds forming in WAP-Epim organoids is inhibited by antibodies against integrin αV. (B) Pie charts showing inhibition of organoid budding in cultures treated with inhibitors of the Map kinase and PI3 kinase pathways, PD098059 and LY294002, respectively. (**C**) Quantification of inhibition of alveolar bud formation in cultures treated with antibodies against integrin αV. **(D)** Quantification of inhibition of alveolar bud formation in both the WT and the WAP-Epim treated with PD098059 or LY294002. **E.** qPCR analysis showing that Pgr upregulation in

the WAP-Epim is abrogated by integrin αV but not by integrin β3 inhibitory antibodies. Bar =75 μM.